ISBN: 978-3-95450-132-8 doi:10.18429/JACoW-IPAC2014-WEPME005

ENHANCED FIELD EMISSION AND EMITTER ACTIVATION ON FLAT DRY-ICE CLEANED CU SAMPLES

S. Lagotzky*, P. Serbun, G. Müller, FB C Physics Department, University of Wuppertal, Germany
T. Muranaka, S. Calatroni, CERN, Geneva, Switzerland

Abstract

Dark currents caused by enhanced field emission (EFE) are considered as major origin of breakdown events limiting performance of pulsed normal conducting Cu accelerating structures. Measurements on diamond-turned, flat Cu samples (R_a = 126 nm) showed first EFE before (after) dry ice cleaning (DIC) at an activation field E_{act} = 130 (190) MV/m. The number density of emitters was significantly reduced by DIC from N = 52.0 cm^{-2} to N = 12.0 cm^{-2} at 190 MV/m. Furthermore, EFE of four diamond-turned and chemically etched Cu samples (Ra = 150 nm) started at 140 MV/m after DIC. Locally measured I(V) curves of the activated emitters yielded onset fields between 20 and 240 MV/m and field enhancement factors up to 350. SEM/EDX investigations revealed surface defects (57%) and few particulates (12%, Al, Si, Sn, W) as origin of the EFE. Moreover, a strong emitter activation effect was observed. A possible breakdown mechanism based on this activation will be discussed.

INTRODUCTION

Electric breakdowns (BD) ignited by field-emitted electrons limit the achievable gradients and cause a severe damage of normal conducting accelerating cavities [1,2]. For the 12 GHz traveling-wave structures of the Compact Linear Collider (CLIC) the maximum allowed breakdown rate (BDR) is 3×10^{-7}/pulse/m at E_{acc} = 100 MV/m [1,3]. Series of prototype structures (E_{peak}/E_{acc} = 2.43) showed that such high field levels are only achievable after long conditioning of the structures (> 1200 h, < 252 ns flat top pulses, 50 Hz) [1,4]. Dark current measurements revealed Fowler-Nordheim (FN) like field dependence with field enhancement factors β_{FN} of 70 (40) before (after) the conditioning [4]. In order to reduce the electron loading and to understand the BD mechanism, we have started to investigate the enhanced field emission (EFE) from flat Cu samples which were fabricated like CLIC accelerating structures. Moreover, the strong EFE suppression of Cu samples by dry ice cleaning (DIC) will be shown.

EXPERIMENTAL DETAILS

Samples

We have used five round (Ø = 12 mm) polycrystalline Cu discs with a hole (Ø = 2 mm) near the edge to identify their position in different measurement systems. All samples were diamond-turned (DT), and four samples got an additional chemical etching (SLAC treatment) which uses a mixture of H_3PO_4 (70.0%), HNO_3 (23.3%), acetic glacial acid (6.6%), and HCl (0.49%) at RT for 5 seconds. Thereby a surface layer of ~ 0.6 µm was removed, and final heating with H_2 at 1040°C was applied, which leads to formation of grains with grain size ≥ 100 µm. Finally, the samples were covered with a Teflon protection cap to avoid any surface damage and particulate contaminations during transport from CERN to Wuppertal.

For the final cleaning of the first sample (only DT) two techniques were tested under cleanroom conditions (class ISO2). At first an ionizing N_2 gun (Simco) at a pressure of 5 bar was used for ~ 1 min. More effort was spent on a DIC system (CryoSnow SJ-10) which provides a round jet of CO_2 snow particles at a propellant gas (N_2) pressure of 8 bar and a liquid CO_2 pressure of 10 bar. The DIC was manually applied under stepwise rotation (4×90°) to sample (cap) for 5 (3) min. The other four samples were directly cleaned by DIC. The protection caps were always removed in the load-lock of the FESM at ~ 10^{-6} mbar.

Measurement Techniques

The EFE measurements were performed with a non-commercial ultra-high vacuum (10^{-9} mbar) field emission scanning microscope (FESM) [5]. Field emitters on the flat samples were localized within an area of 5×5 mm^2 by non-destructive voltage scans V(x,y) for a limited EFE current (I = 1 nA) with an accuracy of 150 µm. In order to achieve a sufficient field homogeneity, the gap between samples and the truncated cone anode (W, Ø = 300 µm) was tilt-corrected within ±1 µm over 1 cm^2. The actual gap width Δz (< 50 µm) was estimated by means of a long-range optical microscope. Depending on the actual EFE current (Keithley 610C), PID-regulated voltages up to 10 kV (FUG HCN100M-10000) were applied to the anode, and electric field maps E(x,y) = V(x,y)/Δz up to 300 MV/m were derived. The resulting number density N of emitters was determined as function of the stepwise increased activation field E_{act}.

For most emitters of the final map, I(V) characteristics were locally measured up to 1 nA (Keithley 6485). The actual local onset field E_{on} was calibrated for each emitter as slope of a PID-regulated V(z) plot for 1 nA. Using the modified Fowler-Nordheim law [6]

$$I_{FN} = A\frac{S_{FN}\beta_{FN}{}^2E^2}{\varphi\, t^2(y)}\exp\left(-B\frac{\varphi^{3/2}v(y)}{\beta_{FN}E}\right) \qquad (1)$$

β_{FN} and the effective emitting area S_{FN} (in cm^2) can be calculated for a given work function φ. For simplicity, we have taken φ = 4.65 eV (Cu), v(y) = t(y) = 1, A = 154, B = 6830 for E in MV/m and I_{FN} in A. Current conditioning

*s.lagotzky@uni-wuppertal.de

Content from this work may be used under the terms of the CC BY 3.0 licence (© 2014). Any distribution of this work must maintain attribution to the author(s), title of the work, publisher, and DOI.

ISBN: 978-3-95450-132-8 doi:10.18429/JACoW-IPAC2014-WEPME005

or ion bombardment of the emitters was not performed yet to keep their original morphology.

In order to reveal the nature of emitters and involved EFE mechanisms, high-resolution scanning electron microscopy (SEM) with energy dispersive x-ray analysis (EDX) was performed (Phillips XL30S) for all locally measured emission sites within a positioning accuracy of ±100 µm. Finally, the average surface quality of the samples in the FESM map regions was determined by means of two-dimensional optical profilometry (OP) with a lateral resolution of 2 µm and height resolution of 3 nm (FRT MicroProf). The linear (square) roughness R_a (R_q) resulting from the OP profiles was 126 (145) nm for the DT surface and 150 (230) nm on average for the additionally etched surfaces.

RESULTS AND DISCUSSION

EFE Activation Statistics

The first stable emitter on the ionized-air-gun cleaned DT sample was activated at E_{act} = 130 MV/m, and finally N = 52.0 ± 14.4 cm^{-2} were obtained at E_{act} = 190 MV/m (Fig. 1). After DIC the sample showed no EFE up to 170 MV/m, and N = 12.0 ± 6.9 cm^{-2} at E_{act} = 190 MV/m was strongly reduced. The etched DIC samples showed first emission at E_{act} = 140 MV/m and N raised to N = 7.0 ± 2.6 cm^2 at E_{act} = 180 MV/m and N = 46.0 ± 6.8 cm^2 at E_{act} = 260 MV/m. On every sample N increased nearly exponentially with the field (N ~ exp(-1/E_{act}) as expected for an exponential N(β) distribution [7]. The validity of this novel N(E_{act}) scaling within statistical errors is demonstrated by the linear fits

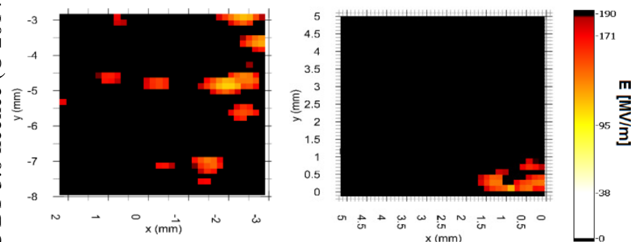

Figure 1: E(x,y) for a DT sample before DIC (left) and for an additionally etched sample after DIC (right) at $E_{act} \leq$ 190 MV/m (area: 5×5 cm^2).

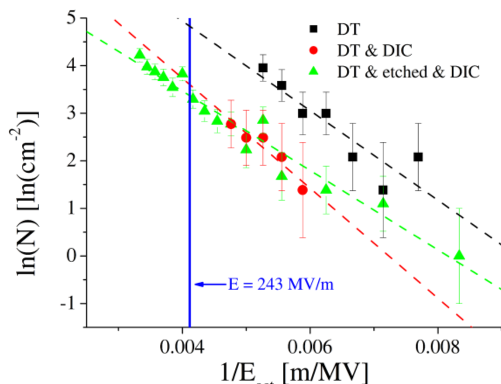

Figure 2: ln(N) vs E_{act}^{-1} and linear fits for three types of samples. The triangles are averaged over four samples.

in Fig. 2. It is remarkable that DIC reduces N at the E_{peak} relevant for CLIC significantly by a factor of 4.2 from N = 124.86 cm^{-2} to N = 29.07 cm^{-2}. The additional etching, however, did not lead to a reduced N at E_{peak}.

Single Emitter Characteristics

Local I(V)-curves were measured for 49 emitters with subsequent SEM/EDX analysis around the emission sites. Altogether 28 surface defects (57 %) and 6 particulates (12 %, Al, Si, Sn, W) with a diameter between 200 nm & 2 µm were found as most probable features causing EFE. For the remaining 15 emitters an identification of the EFE origin was impossible due to emitter destruction [5] or the presence of both, surface defects and particulates [8]. Typically, surface defects, e.g. scratches, lead to a rather stable FN-like EFE (Fig. 3a) with slight jumps and some hysteresis most probably caused by melting of micro-tips. Particulates, however, tend to cause a more unstable EFE, sometimes with a changed slope at high fields (Fig. 3b) due to a bad electrical contact to the bulk material. Both types of emitters mainly reveal β_{FN}-values in the range of

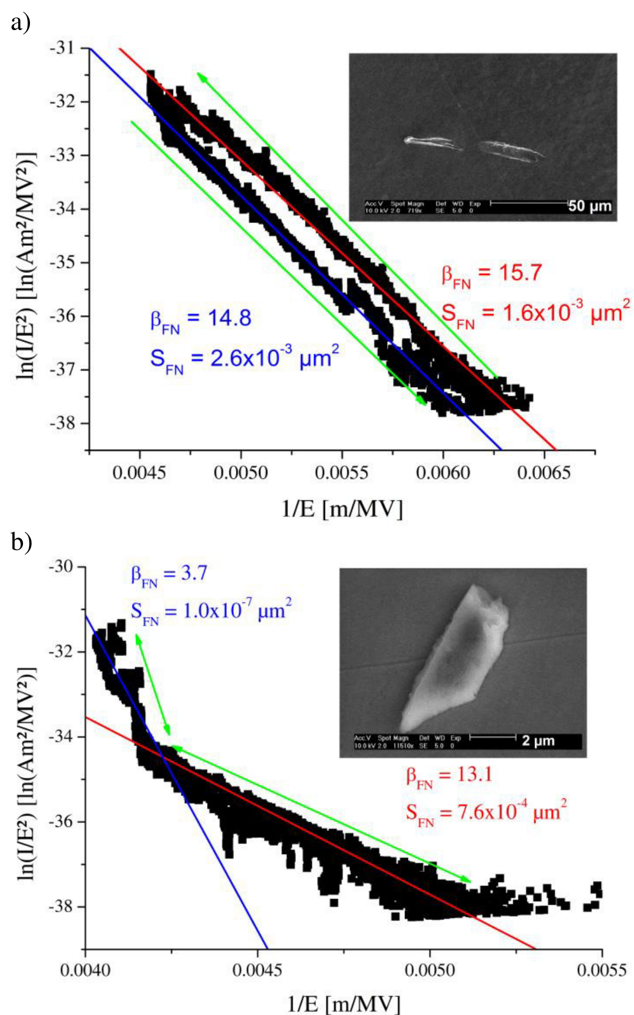

Figure 3: Typical FN-plots and SEM images (insets) of a (a) surface defect and (b) particulate (Al, Si). The arrows indicate up and down swing of E. Please note the β_{FN} and S_{FN} resulting from the line fits.

Content from this work may be used under the terms of the CC BY 3.0 licence (© 2014). Any distribution of this work must maintain attribution to the author(s), title of the work, publisher, and DOI.

ISBN: 978-3-95450-132-8 doi:10.18429/JACoW-IPAC2014-WEPME005

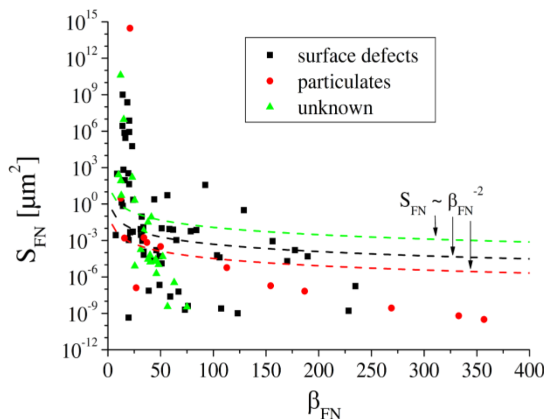

Figure 4: Correlation between S_{FN} and β_{FN} of the locally measured emitters on all Cu samples. The dashed fit lines correspond to geometrical field enhancement.

10-70 with some exceptions (~15%) in the high-β_{FN} range (β_{FN} > 150) caused by particulates and scratches, but not by emission sites with unknown origin (see Fig. 4). It is remarkable, that the highest β_{FN} values are caused by particulates. Most S_{FN} values are in a reasonable range of 10^{-9}-10^{-3} µm^2 for all three types of emitters. The corresponding β_{FN} and S_{FN} data are barely correlated as expected for geometrical field enhancement ($S_{FN} \sim \beta_{FN}^{-2}$). Unreasonably high S_{FN} values with respect to anode size (> 7×10^4 µm^2) were observed in the low-β_{FN} range (< 25). This clearly hints for other emission mechanisms besides geometrical field enhancement to be involved in the EFE of Cu samples, e.g. MIV-emission in case of surface defects or MIM-emission in case of particulates [9].

In accordance to their activation, all emitters yielded a significantly reduced onset field $E_{on} < E_{act}$ for an emission current of 1 nA, similar to emitters on Nb [8]. As shown in Fig. 5, the values of E_{on} vary between 20 – 240 MV/m (40 – 240 MV/m) for scratches (particulates). Therefore, both types of emitters can lead to strong electron loading

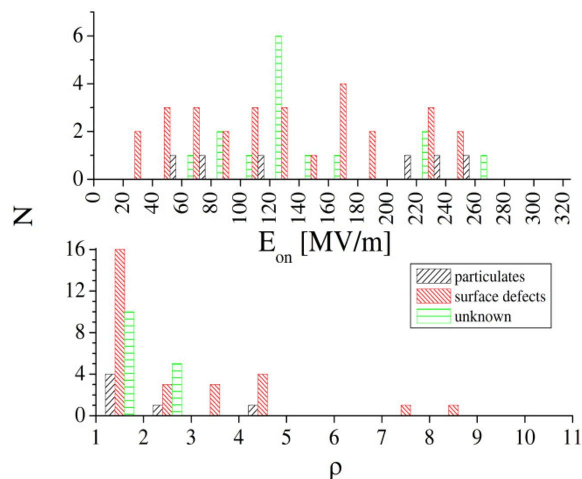

Figure 5: Histograms of N as function of E_{on} (top) and ρ (bottom) for the different types of emitters.

of cavities if activated. A useful measure for the activation strength is the field reduction factor $\rho = E_{act}/E_{on}$. For most emitters (61%) it is ρ ≤ 2 but some emitters (20%) provide ρ ≥ 3 (Fig. 5). It is remarkable that the two highest ρ-values (8.89 & 7.95) and 90% of the emission sites with ρ ≥ 3 are caused by surface defects. These high-ρ emitters are most likely candidates for triggering BD in normal conducting accelerating structures because of the exponential current increase after activation during a rf pulse. The emitter with the highest ρ value, for example, was activated at E_{act} = 240 MV/m to E_{on} = 27 MV/m and would emit I ~ 5 A (β_{FN} = 189.5, S_{FN} = 4.87×10^{-5} µm^2, j ~ 1×10^{13} A/cm^2) at the maximum E_{peak} = 243 MV/m. Therefore, such a strong activation would surely cause an emitter explosion and a BD of the cavity field.

CONCLUSIONS

The EFE from flat Cu samples is dominated by particulates and surface defects, and N can be significantly decreased (factor ~ 4 at E_{peak}) by DIC which mainly removes particulates. Nevertheless, even after DIC, and extrapolating to CLIC RF structures, there are still ~ 30 emitters in the high-field area around the iris (~ 1 cm^2 with E ≥ 0.95×E_{peak}) of each accelerating cell, and 20% of these emitters might cause a BD due to their high ρ-value. Most of these emitters are surface defects which remain on the surface even after chemical etching. Moreover, geometrical field enhancement is not sufficient to explain the observed EFE from smooth Cu surfaces. Alternative emission processes like the MIV- and MIM-model should also be considered.

In the next test series we will focus on removing the few remaining particulates by optimization of the DIC, and on minimizing surface defects on the Cu samples.

ACKNOWLEDGMENT

We thank A. Korsback for providing the samples and Dr. R. Heiderhoff for access to the SEM/EDX facility at FB E of University of Wuppertal. The work is funded by BMBF project 05H12PX6.

REFERENCES

[1] CLIC Conceptual Design Report, CERN-2012-007.
[2] H. H. Braun et al., MPPH039, Proc. PAC2001.
[3] A. Grudiev et al., THP062, Proc. LINAC08.
[4] T. Higo et al., THPEA012, Proc. IPAC10.
[5] D. Lysenkov and G. Müller, Int. J. Nanotechnol. 2, 239 (2005).
[6] R. G. Forbes, J. Vac. Sci. Technol. B 17, 526 (1999).
[7] S. Lagotzky, G. Müller, WEPME004, IPAC14.
[8] A. Navitski et al., Phys. Rev. ST Accel. Beams 16, 112001 (2013).
[9] R. V. Latham, High Voltage Vacuum Insulation, Academic Press, London (1995).

Content from this work may be used under the terms of the CC BY 3.0 licence (© 2014). Any distribution of this work must maintain attribution to the author(s), title of the work, publisher, and DOI.